Membrane Transport, Structure, Function, and Biogenesis:

Cystic Fibrosis Transmembrane Conductance Regulator-independent Phagosomal Acidification in Macrophages

Peter M. Haggie and A. S. Verkman

J. Biol. Chem. 2007, 282:31422-31428.
doi: 10.1074/jbc.M705296200 originally published online August 27, 2007

THE JOURNAL OF BIOLOGICAL CHEMISTRY VOL. 282, NO. 43, pp. 31422–31428, October 26, 2007

Cystic Fibrosis Transmembrane Conductance Regulator-independent Phagosomal Acidification in Macrophages*

Received for publication, June 28, 2007, and in revised form, August 23, 2007 Published, JBC Papers in Press, August 27, 2007, DOI 10.1074/jbc.M705296200

Peter M. Haggie and A. S. Verkman[1]

From the Departments of Medicine and Physiology, University of California, San Francisco, California 94143-0521

It was reported recently that the cystic fibrosis transmembrane conductance regulator (CFTR) is required for acidification of phagosomes in alveolar macrophages (Di, A., Brown, M. E., Deriy, L. V., Li, C., Szeto, F. L., Chen, Y., Huang, P., Tong, J., Naren, A. P., Bindokas, V., Palfrey, H. C., and Nelson, D. J. (2006) *Nat. Cell Biol.* 8, 933–944). Here we determined whether the CFTR chloride channel is a generalized pathway for chloride entry into phagosomes in macrophages and whether mutations in CFTR could contribute to alveolar macrophage dysfunction. The pH of mature phagolysosomes in macrophages was measured by fluorescence ratio imaging using a zymosan conjugate containing Oregon Green® 488 and tetramethylrhodamine. Acidification of phagolysosomes in J774A.1 macrophages (pH ~5.1 at 45 min), murine alveolar macrophages (pH ~5.3), and human alveolar macrophages (pH ~5.3) was insensitive to CFTR inhibition by the thiazolidinone $CFTR_{inh}$-172. Acidification of phagolysosomes in alveolar macrophages isolated from mice homozygous for ΔF508-CFTR, the most common mutation in cystic fibrosis, was not different compared with that in alveolar macrophages isolated from wild-type mice. We also measured the kinetics of phagosomal acidification in J774A.1 and murine alveolar macrophages using a zymosan conjugate containing fluorescein and tetramethylrhodamine. Phagosomal acidification began within 3 min of zymosan binding and was complete within ~15 min of internalization. The rate of phagosomal acidification in J774A.1 cells was not slowed by $CFTR_{inh}$-172 and was not different in alveolar macrophages from wild-type *versus* ΔF508-CFTR mice. Our data indicate that phagolysosomal acidification in macrophages is not dependent on CFTR channel activity and do not support a proposed mechanism for cystic fibrosis lung disease involving defective phagosomal acidification and bacterial killing in alveolar macrophages.

Chronic lung infection and deterioration of lung function are the major causes of morbidity and death in cystic fibrosis (CF)[2] (1, 2). Although the genetic defect in CF was identified in 1989 (mutations in the gene encoding the cystic fibrosis transmembrane conductance regulator (CFTR)), the mechanisms by which CFTR mutations cause lung disease remain uncertain. Various mechanisms have been proposed to link defective CFTR function to CF lung disease, such as defective airway submucosal gland secretion, abnormal airway surface liquid composition or oxygenation, Na^+ hyperabsorption producing airway surface liquid dehydration (reduced airway surface liquid volume), loss of CFTR regulation of other transport proteins, and intrinsic hyperinflammation (reviewed in Refs. 3–6). Determination of the mechanisms linking defective CFTR function to CF lung disease is of great importance in developing rational therapies to treat CF.

A recent report of defective phagolysosomal acidification in alveolar macrophages in CFTR null mice suggested a new mechanism to link defective CFTR function to CF lung disease (7). Macrophages are key protagonists of the innate immune system and patrol the body, including the alveolar surface, to engulf and destroy pathogens in their phagolysosomes (8–10). Di *et al.* (7) reported that phagolysosomes in alveolar macrophages acidify in a CFTR-dependent manner and that defective acidification of phagolysosomes in alveolar macrophages from CFTR null mice impairs their bactericidal activity. It is interesting that no defect in bactericidal activity was observed in peritoneal macrophages from CFTR null mice, suggesting that CFTR-dependent acidification of phagolysosomes is specific to alveolar macrophages. Although the authors made no direct connection between CFTR mutations, acidification of phagosomes in alveolar macrophages, and CF disease progression, the prevailing view has emerged that defective alveolar macrophage function is important in the pathophysiology of CF lung disease (11–13).

Here we use ratiometric, fluorescent zymosan and dextran conjugates to determine the role of CFTR in the acidification of phagolysosomes in macrophages. In J774A.1 macrophages, phagolysosomal and lysosomal acidification was not dependent upon CFTR chloride conductance. We also found that phagolysosomal acidification was not dependent on CFTR channel activity in murine and human alveolar macrophages and was

* This work was supported by National Institutes of Health Grants HL73856, HL59198, EB00415, DK35124, and EY13574; Research and Translational Core Center Grant DK72517; and Research Development Program and Drug Discovery grants from the Cystic Fibrosis Foundation. The costs of publication of this article were defrayed in part by the payment of page charges. This article must therefore be hereby marked "*advertisement*" in accordance with 18 U.S.C. Section 1734 solely to indicate this fact.

[1] To whom correspondence should be addressed: Cardiovascular Research Inst., University of California, 1246 Health Sciences East Tower, P. O. Box 0521, San Francisco, CA 94143-0521. Tel.: 415-476-8530; Fax: 415-665-3847; E-mail: alan.verkman@ucsf.edu.

[2] The abbreviations used are: CF, cystic fibrosis; CFTR, cystic fibrosis transmembrane conductance regulator; TMR, tetramethylrhodamine; PBS, phosphate-buffered saline.

not different in ΔF508-CFTR murine alveolar macrophages. As such, CFTR channel activity is not required for phagosomal acidification in macrophages.

EXPERIMENTAL PROCEDURES

Cells—J774A.1 murine macrophages (ATCC TIB-67), which are of peritoneal origin, were cultured in Dulbecco's modified Eagle's medium H-21 using standard procedures. Alveolar macrophages were freshly isolated from wild-type and CF (ΔF508-CFTR homozygous) mice in a CD1 genetic background. Briefly, mice were killed by intraperitoneal injection of ketamine, and alveolar macrophages were obtained immediately by bronchoalveolar lavage (7, 14). Mice were provided by the CF Animal Core Facility of the University of California, San Francisco. Human alveolar macrophages were obtained by lavage of lungs that were rejected for lung transplantation as part of the California Transplant Program. Alveolar macrophages were identified by standard morphological criteria and confirmed by the uptake of non-opsonized zymosan.

Fluorescent Probe Synthesis—Ratioable, pH-sensitive, fluorescent probes for measurement of phagolysosomal and lysosomal pH were synthesized using standard succinimidyl ester chemistry. Oregon Green® 488-X or 5(6)-carboxyfluorescein was covalently coupled to zymosan (Sigma) together with tetramethylrhodamine (TMR). For lysosomal pH determination, Oregon Green® 488-X and TMR were conjugated to 40-kDa amino dextran (Invitrogen). For each probe, TMR is a pH-insensitive marker of conjugate uptake to allow ratio imaging.

Cell Labeling, in Situ Calibration, and Quantitative Fluorescence Imaging—For measurement of the pH of mature phagolysosomes, cells were incubated with 0.5 mg/ml Oregon Green® 488/TMR-zymosan for 30–45 min at 37 °C in phosphate-buffered saline (PBS) supplemented with 6 mM glucose and 1 mM pyruvate (PBS/Glc/Pyr), washed three to five times with PBS, and imaged. To label lysosomes, cells were incubated with 4–10 mg/ml Oregon Green® 488/TMR-dextran for 30 min at 37 °C in PBS/Glc/Pyr, washed, and incubated in PBS/Glc/Pyr for 2 h at 37 °C to chase dextran to lysosomes. The kinetics of phagosomal acidification was measured using a method based on published protocols to synchronize the uptake of phagocytic substrates (12, 15, 16). Cells were washed with 4 °C PBS/Glc/Pyr and incubated with 0.5 mg/ml 5(6)-carboxyfluorescein/TMR-zymosan at 4 °C for 20–30 min. 5 volumes of 37 °C PBS/Glc/Pyr were then added to the cells, and internalization of 5(6)-carboxyfluorescein/TMR-zymosan was allowed to proceed for 2 min at 37 °C before washing the cells four times with 4 °C PBS/Glc/Pyr to remove zymosan that had not internalized. Cells were kept at 4 °C for up to 2 h prior to experiments. The temperature was raised to 37 °C just prior to microscopy, and initial images were acquired 3 min after internalization began. All imaging experiments were performed in PBS/Glc/Pyr. In some experiments, the thiazolidinone CFTR inhibitor $CFTR_{inh}$-172 was used at 10 μM, or the vacuolar ATPase inhibitor bafilomycin A_1 was used at 100 nM. Inhibitors were present during cell loading, chase, and experiments.

In situ calibration experiments were done to relate fluorescence ratios to pH. After loading (as described above), cells with labeled phagolysosomes or lysosomes were incubated for 30–40 min at 37 °C in calibration buffer (5 mM Hepes, 5 mM potassium citrate, 120 mM KCl, 20 mM NaCl, 1 mM $CaCl_2$, 1 mM $MgCl_2$, 100 nM bafilomycin A_1, 10 μM nigericin, 10 μM valinomycin, and 10 μM carbonyl cyanide *m*-chlorophenylhydrazone) at pH 2.5–8.6. Background-corrected fluorescence ratios at different pH values were fitted to the following equation: $F_{green}/F_{red} = A + B((1 + 10^{(pK_a - pH)n_H})^{-1})$.

Microscopy—Fluorescence images were acquired on a Nikon TE2000U microscope equipped with a 100×/numerical aperture 1.45 Plan Apo TIRF objective, an EXFO X-Cite light source, a Hamamatsu EM-CCD camera, a UNIBLITZ shutter, and a microincubator to maintain cells at 37 °C during data acquisition. Sequential, wide-field images of cells were captured using Chroma 31001 and 31002 filter sets. Neutral density filters were placed in the excitation light path to attenuate illumination intensity, and the absence of photobleaching was confirmed in control experiments by stable fluorescence of labeled cells during continuous illumination. For kinetic experiments, illumination light was shuttered in between data acquisition. Images of representative cells containing phagocytosed Oregon Green® 488/TMR-zymosan were obtained using a Nikon TE2000S microscope equipped for phase-contrast and fluorescence imaging and a Hamamatsu EM-CCD camera. Cells were incubated with fluorescent zymosan for 45 min and fixed in 4% paraformaldehyde in PBS prior to imaging. As we reported in prior studies of endosomal pH and chloride (17–19), standard image analysis was performed by computing area-integrated, background-subtracted fluorescence intensities for specified regions of interest using NIH ImageJ software.

RESULTS

To measure the pH of mature phagolysosomes, we synthesized a fluorescent pH indicator consisting of Oregon Green® 488 (pK_a ~4.7) and TMR covalently bound to zymosan (Fig. 1*A*, *inset*). The pK_a of Oregon Green® 488 renders it pH-sensitive at or near the acidic pH of mature macrophage phagolysosomes and allows accurate measurement of phagolysosomal pH by two-color ratio imaging. Unlike Di *et al.* (7), we chose a ratiometric approach to measure phagosomal pH such that our measurements were insensitive to probe concentration. To calibrate the pH probe, we incubated J774A.1 macrophages with the zymosan conjugate for 45 min to allow internalization of the probe and subsequent maturation of phagolysosomes. Labeled cells were then washed and exposed to solutions at the specified pH containing ionophores to equilibrate the extracellular and intraphagosomal pH. The pK_a determined for Oregon Green® 488 by ratio imaging of cells at different pH values agreed with that determined *in vitro* (Fig. 1*A*), indicating that the zymosan conjugate faithfully reports phagolysosomal pH.

We initially measured the pH of phagolysosomes in J774A.1 murine macrophages, which were reported previously to express CFTR by biochemical, electrophysiological, and immunocytochemical criteria (7). Following incubation of J774A.1 macrophages with fluorescent zymosan, fluorescently labeled phagolysosomes were seen through the green and red channels as shown in Fig. 1*B*, which are shown along with a pH pseudocolored ratio image. The intensity of individual phagolysosomes varied greatly, indicating that zymosan uptake and/or

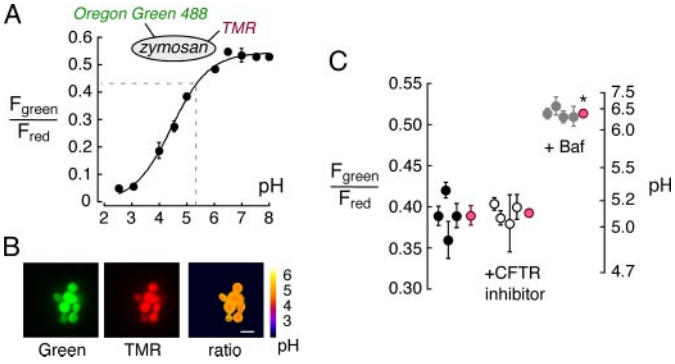

FIGURE 1. **Phagolysosomal acidification in J774A. 1 macrophages is not dependent on CFTR chloride channel function.** *A, in situ* calibration of a zymosan conjugate containing Oregon Green® 488 and TMR (*inset*). J774A.1 macrophages were labeled with fluorescent zymosan, and the probe fluorescence ratio (F_{green}/F_{red}) was measured using perfusates at the specified pH containing high K^+/ionophores (see "Experimental Procedures"). Average data are shown for three separate experiments at each calibration point, with 20–63 phagosomal regions analyzed per experiment. Phagolysosomal pH from one experiment is overlaid on the calibration curve (*dashed line* on calibration curve). *B*, fluorescence micrographs of labeled J774A.1 macrophages showing Oregon Green® 488 (*green*) and TMR (*red*) fluorescence and a pseudocolored ratio image. *Scale bar* = 5 μm. *C*, phagolysosomal pH in J774A.1 macrophages measured by ratio imaging. pH values for individual control experiments (*black circles*) and the mean ± S.E. for the data sets (*red circles*) are shown. Where indicated, $CFTR_{inh}$-172 (10 μM; *white circles*) or bafilomycin (*Baf*; 100 nM; *gray circles*) was included during incubations. *, $p <$ 0.001 by analysis of variance with the Bonferroni post hoc test. 25–112 phagolysosomal regions were analyzed per experiment.

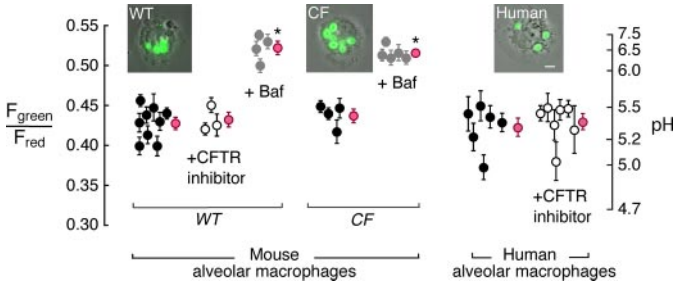

FIGURE 2. **Phagolysosomal acidification in murine and human alveolar macrophages is not dependent on CFTR chloride channel function.** Phagolysosomal pH was measured by ratio imaging, and pH values for individual control experiments (*black circles*) and the mean ± S.E. for data sets (*red circles*) are shown. Where indicated, $CFTR_{inh}$-172 (10 μM; *white circles*) or bafilomycin (*Baf*; 100 nM; *gray circles*) was included during incubations, and alveolar macrophages from ΔF508-CFTR mice were studied. *, $p < 0.001$ by analysis of variance with the Bonferroni post-hoc test. 28–146 phagolysosomal regions were analyzed per experiment. *Insets* show phase-contrast images of paraformaldehyde-fixed murine and human macrophages with overlaid fluorescence from phagolysosomes. *Scale bar* = 5 μm. *WT*, wild-type.

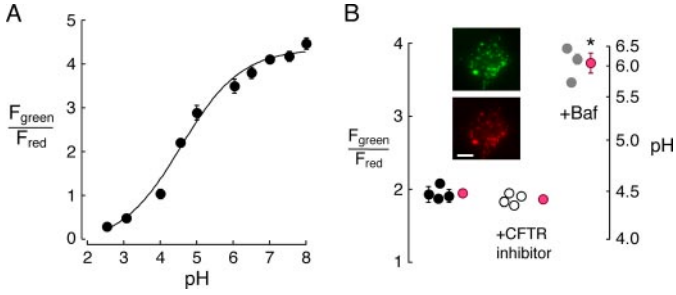

FIGURE 3. **Lysosomal pH in J774A.1 macrophages is not dependent on CFTR chloride channel activity.** *A*, *in situ* calibration of a 40-kDa dextran conjugate containing Oregon Green® 488 and TMR. J774A.1 macrophages were labeled with fluorescent dextran for 30 min, followed by 2-h chase at 37 °C to allow probe accumulation in lysosomes. Calibration of F_{green}/F_{red} *versus* pH was done using solutions at the specified pH containing high K^+/ionophores. Average data are shown for three separate experiments at each calibration point, with 21–103 lysosomal regions analyzed per experiment. *B*, lysosomal pH in J774A.1 macrophages determined by ratio imaging. pH values for individual control experiments (*black circles*) and the mean ± S.E. for data sets (*red circles*) are shown. Where indicated, $CFTR_{inh}$-172 (10 μM; *white circles*) or bafilomycin (*Baf*; 100 nM; *gray circles*) was included during incubations. *, $p < 0.001$ by analysis of variance with the Bonferroni post hoc test. 35–89 lysosomal regions were analyzed per experiment. *Insets* show fluorescence images of J774A.1 macrophages. *Scale bar* = 5 μm.

size varies in phagosomes. Averaged data for many cells indicated that phagolysosomes attained an acidic pH of 5.08 ± 0.08 (Fig. 1*C*, *left*), in agreement with previous studies (12, 20, 21). To assess the CFTR dependence of phagolysosomal acidification in J774A.1 macrophages, we labeled cells with Oregon Green® 488/TMR-zymosan in the presence of 10 μM $CFTR_{inh}$-172, a selective inhibitor active against CFTR from different species, including human and mouse (22). Phagolysosomal acidification was insensitive to the CFTR inhibitor in J774A.1 macrophages with a final pH of 5.10 ± 0.03 (Fig. 1*C*, *middle*). To confirm that our fluorescent indicator was sensitive to pH changes, phagolysosomal pH was measured following incubation with bafilomycin A_1, an inhibitor of the vacuolar ATPase required for phagosomal acidification (15). As expected, phagolysosomes failed to acidify completely, reaching a pH of ~6.5 (Fig. 1*C*, *right*), in agreement with previous data (15, 20).

To determine the role of CFTR channel activity in the acidification of phagolysosomes in alveolar macrophages, similar measurements were done in alveolar macrophages lavaged from mouse lungs. In alveolar macrophages from wild-type mice, phagolysosomal acidification was not impaired by the CFTR inhibitor (pH 5.34 ± 0.05 *versus* 5.37 ± 0.07) (Fig. 2, *left*). Furthermore, phagolysosomal pH in alveolar macrophages from CF mice containing the most common CF mutation, ΔF508-CFTR, was not significantly different from that in alveolar macrophages from wild-type mice (pH 5.34 ± 0.05 *versus* 5.40 ± 0.06) (Fig. 2, *middle*). As expected, phagolysosomal acidification was sensitive to bafilomycin (Fig. 2, *left* and *middle*), confirming dependence on the vacuolar H^+-ATPase. We also found that the CFTR-selective inhibitor $CFTR_{inh}$-172 did not impair acidification of phagolysosomes in (non-CF) human alveolar macrophages (pH 5.30 ± 0.08 *versus* 5.35 ± 0.07) (Fig. 2, *right*).

To account for their finding of defective phagolysosomal acidification in CF alveolar macrophages, Di *et al.* (7) reported that (i) lysosomal acidification is defective in CFTR knock-out macrophages and that (ii) lysosomal fusion to phagosomes is responsible for phagolysosomal acidification. To assess whether lysosomal acidification is dependent on CFTR channel activity, we measured lysosomal acidification in J774A.1 macrophages using a dextran conjugate containing Oregon Green® 488 and TMR. This ratiometric, fluid-phase marker was sensitive at the acidic pH values found in lysosomes (Fig. 3*A*). Lysosomes were labeled by a standard pulse-chase protocol (Fig. 3*B*, *inset*). We found that lysosomal acidification in J774A.1 murine macrophages was not altered by the CFTR inhibitor $CFTR_{inh}$-172 at 10 μM (pH 4.48 ± 0.03 *versus* 4.42 ± 0.03). In a control study, lysosomes failed to acidify completely in the presence of bafilomycin (Fig. 3*B*).

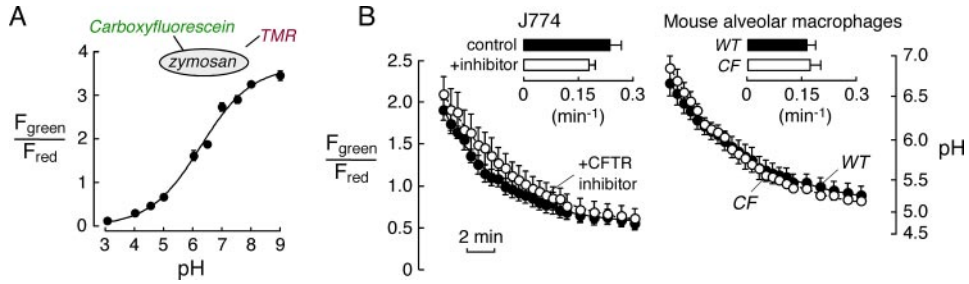

FIGURE 4. **CFTR-independent phagosomal acidification kinetics in J774A.1 and alveolar macrophages.** *A*, *in situ* calibration of a zymosan conjugate containing fluorescein and TMR (*inset*). Average data are shown for four to five separate experiments at each calibration point, with 22–64 phagosomal regions analyzed per experiment. *B*, acidification kinetics of phagosomes in J774A.1 macrophages (*left*) and murine alveolar macrophages (*right*). Cells were pulse-labeled with the zymosan conjugate, and initial images of phagosomes were taken 3 min after initiation of phagocytosis. Where indicated, J774A.1 macrophages were incubated with $CFTR_{inh}$-172 (10 μM; *left*, *open circles*), and murine macrophages from ΔF508-CFTR mice (*right*, *open circles*) were studied. *Insets* show averaged rate constants (mean ± S.E. for four to five separate experiments, with three to eight phagosomal regions analyzed per experiment). Differences were not significant. *WT*, wild-type.

Using live cell imaging, Di *et al.* (7) reported that phagosomal acidification occurs after fusion with lysosomes but that this fusion event occurs 20–30 min after an initial zymosan acidification event (~0.5 pH units lower than cytoplasmic or external pH; see "Discussion"). In the case of CFTR null macrophages, although fusion of lysosomes to phagosomes was observed, acidification did not occur, as lysosomes are not acidic. To reassess these unexpected findings, we measured the kinetics of phagosomal acidification using a zymosan conjugate containing 5(6)-carboxyfluorescein (pK_a ~6.4) and TMR (Fig. 4*A*, *inset*). This zymosan conjugate was chosen to more accurately report the initial stages of phagosomal acidification as compared with the Oregon Green® 488 conjugate, the signal of which becomes saturated above pH ~7, as shown in Fig. 1*A*. Following pulse label-chase, phagosomal acidification in J774A.1 macrophages (Fig. 4*B*, *left*) and murine alveolar macrophages (*right*) began within 3 min of phagocytosis and reached steady state by ~15 min, in agreement with previous data obtained with murine peritoneal and bone marrow-derived macrophages (15, 21), although contrary to the kinetic data of Di *et al.* (7). Furthermore, the rate of acidification in J774A.1 macrophages was not altered by CFTR inhibition by $CFTR_{inh}$-172, nor was rate of acidification different in wild-type *versus* ΔF508-CFTR alveolar macrophages (Fig. 4*B*). The final pH values obtained using 5(6)-carboxyfluorescein/TMR-zymosan were in good agreement with those determined using Oregon Green® 488/TMR-zymosan. Taken together, these data indicate that phagolysosomal acidification in macrophages is not dependent on CFTR chloride channel activity.

DISCUSSION

The aim of this study was to investigate the role of CFTR channel activity in phagosomal acidification in macrophages. Our study was motivated by the critical role for CFTR in phagosomal acidification as reported recently (7) and the important implications of this finding to bacterial killing by alveolar macrophages and mechanisms of CF lung disease. A CFTR-dependent defect in the acidification of lysosomes and phagolysosomes (by 1–2 pH units) in alveolar, but not peritoneal, macrophages from CFTR null mice was reported to be responsible for reduced bacterial killing (7). Using the CFTR inhibitor $CFTR_{inh}$-172, we found pharmacological evidence against CFTR involvement in phagosomal acidification in J774A.1 macrophages and in murine and human alveolar macrophages. Furthermore, using alveolar macrophages isolated from ΔF508-CFTR mice, we found no evidence for defective phagolysosomal acidification with mutant CFTR. As such, our experimental approach does not formally rule out the possibility that residual channel activity from ΔF508-CFTR or after CFTR inhibition is responsible for the observed acidification in phagosomes and lysosomes. However, for several reasons, we believe that significant residual channel activity is unlikely. The targeting of ΔF508-CFTR to phagosomal membranes is very unlikely given that this mutant resides in the endoplasmic reticulum (2, 23, 24), and a complete absence of endoplasmic reticulum-derived components in phagosomes has been proven (25). Furthermore, ΔF508-CFTR is strongly inhibited at acidic pH (26), is subject to degradation in lysosomes (27), and requires a chemical potentiator (such as genistein) to produce significant chloride channel activity (28). For experiments with the inhibitor $CFTR_{inh}$-172 (used at 10 μM), which has an IC_{50} of ~300 nM, complete CFTR inhibition has been found at ~5–10 μM in a variety of cellular and tissue preparations (22, 29). Finally, we cannot formally rule out the unlikely possibility that CFTR performs an alternative function, other than ion conductance, that has not been directly assessed by our studies. For example, CFTR has been reported to participate in the regulation of endocytosis, exocytosis, and endosomal fusion (30, 31). However, taken together, our data indicate that CFTR does not constitute a universal pathway for chloride ion conductance in the phagosomal or lysosomal membranes of macrophages, and so defective acidification of alveolar macrophage phagosomes does not contribute to CF disease progression in CF subjects with the common ΔF508-CFTR mutation.

The mechanism of phagosomal maturation in macrophages is incompletely understood; however, a variety of biophysical, proteomic, and genetic approaches have begun to elucidate this process (10, 32, 33). To the best of our knowledge, in all studies that rigorously investigated the kinetics of phagosomal acidification, irrespective of macrophage origin or the precise assay protocol, acidification of phagosomes to ~pH 5 was observed to begin within 2–3 min of probe binding and was complete within 5–15 min of particle ingestion (12, 15, 16, 20, 21, 34). Phagosomal acidification in macrophages is mediated by the bafilomycin-sensitive vacuolar ATPase (15, 16); however, there is no consensus on the cellular source for delivery of this proton pump to phagosomes. Indeed, vacuolar ATPases are found in many cellular membranes, including the plasma membrane, early endosomes, and the Golgi (35). Several studies have indicated, however, that lysosomes are probably not the source of

vacuolar ATPase for phagosomal acidification. In murine peritoneal macrophages, phagosomal acidification is complete prior to fusion with lysosomes, as assessed by fluorescence imaging and electron microscopy (15). Electron microscopy of J774A.1 macrophages (in which phagosomes acidify rapidly after particle ingestion (Ref. 20 and this study)) indicated that lysosomal fusion to phagosomes is not observed until >10 min after phagocytic uptake (Fig. 2 in Ref. 36). Live cell fluorescence microscopy of RAW 264.7 macrophages (in which phagosomes acidify rapidly after particle ingestion (12)) also demonstrated that the lysosomal marker LAMP-1 is not enriched on phagosomes until ~20 min after particle ingestion (37). Finally, in bone marrow-derived macrophages, fluorescence resonance energy transfer-based assays of lysosomal/phagosomal fusion indicated that fusion lags behind acidification by 5–10 min (21, 34). Thus, a large body of data indicates that macrophage phagosomes acidify rapidly after particle ingestion and that lysosomal contents are delivered to the maturing phagosome some time (≥10 min) after acidification has initiated (10). As such, our measurements of the rates of phagosomal acidification are in accord with previously published data.

In contrast to this consensus mechanism, Di *et al.* (7) reported that mouse alveolar macrophages maintain zymosan particles at pH ~6.8 (~0.5 pH units lower than extracellular or cytoplasmic pH) for 20–30 min prior to complete phagosomal acidification, which occurs only after lysosomal fusion and delivery of acidic contents. The data of Di *et al.* do not clearly indicate the time of zymosan uptake (Fig. 7 and associated movies in Ref. 7). As such, it is not clear why zymosan initially reports pH <7. Furthermore, as no statistics were provided for these experiments, it is not possible to assess the generality of this observation.

Major differences between this work and the study of Di *et al.* (7) exist in the methods used to measure phagolysosomal and lysosomal pH. Whereas we used a ratiometric approach with pH-sensitive (Oregon Green® 488 or fluorescein) and pH-insensitive (TMR) dyes conjugated to zymosan, Di *et al.* relied upon a single pH-sensitive fluorophore (fluorescein) and no marker of probe uptake. Single wavelength determination of pH has been reported (38, 39); however, such applications relied upon post-calibration of fluorescence intensity with high K^+/ionophore-containing solutions, which does not appear to have been done by Di *et al.* (7). Ratiometric methods are clearly preferable to single wavelength methods in the determination of physiological parameters such as pH and Ca^{2+} (40, 41). In terms of the fluorophores used in the respective studies, maximum sensitivity is afforded when the pK_a of a fluorophore is similar to the pH of the compartment being investigated. In the case of phagosomes and lysosomes (pH 4.5–5.3), Oregon Green® 488 (pK_a ~4.7) is a much superior fluorophore compared with fluorescein (pK_a ~6.5) for steady-state pH measurements. For measurements of phagosomal acidification rate (Fig. 4), fluorescein was chosen as a pH probe because the initial pH in early phagosomes is >7, where the Oregon Green® 488 fluorescence signal is saturated. Despite the relatively lower sensitivity of fluorescein at ~pH 5, our measurements of final pH in phagosomes using fluorescein/TMR-zymosan (Fig. 4) were in excellent agreement with the steady-state measurements (Figs. 1 and 2). For lysosomes, a pH of ~4.5 was reported in this study and by Di *et al.* (7); such acidic pH quenches fluorescein fluorescence by ~95%, rendering this dye quite insensitive. Furthermore, Di *et al.* (7) used confocal microscopy to image samples, whereas we relied upon wide-field detection. Because of the substantial height of macrophages (~10–15 μm), the intrinsic optical sectioning of confocal microscopy (42), and the mobility of phagosomes (36, 43), movement and chromatic artifacts can confound quantitative imaging applications done at a single wavelength.

Using several assays, Di *et al.* reported that alveolar, but not peritoneal, macrophages from CFTR null mice are less efficient at bacterial killing than those from wild-type mice (Fig. 3 in Ref. 7). In addition to assessing phagolysosomal pH, several additional processes necessary for bacterial killing by macrophages were assessed to determine the mechanism by which CFTR-dependent defects impair killing (7). The generation of oxidative species by macrophages was assessed by fluorescence imaging of CFTR null and wild-type cells loaded with 2′,7′-dichlorodihydrofluorescein diacetate (7). This probe is readily taken up by cells and is ultimately oxygenated to generate the fluorescent species 2′,7′-dichlorofluorescein, the intensity of which is generally taken to be a readout of reactive oxygen species activity. Di *et al.* reported that the intensity of 2′,7′-dichlorofluorescein in phagolysosomes from CFTR null mice is identical to that from wild-type mice (Fig. S2 in Ref. 7). However, 2′,7′-dichlorofluorescein is pH-sensitive (pK_a ~5), such that their measured pH of phagolysosomes in CFTR null (pH ~6.5) *versus* wild-type (pH ~4.7) mice would confound interpretation of these data. Indeed, the quenching of 2′,7′-dichlorofluorescein by the acidic environment of phagosomes in wild-type mice relative to that in CFTR null mice would account for a significant difference in fluorescence signal, suggesting that wild-type mice produce much more reactive oxygen species than CFTR null mice. A role for CFTR in transport of chloride ions into neutrophil phagosomes for the generation of oxidative species was recently proposed (44). As such, the mechanism of CFTR-dependent bacterial killing in CFTR null macrophages warrants further, definitive investigation.

There is long-standing interest concerning the possibility of defective organellar acidification in CF cells. Defective acidification (by ~0.25 pH units) of the *trans*-Golgi, endosomes, and prelysosomes in CF was initially reported by Al-Awqati and co-workers (45), suggesting a role for CFTR in organellar counterion conductance. This work was subsequently refuted by multiple laboratories (46–50). Of direct relevance to this study, CFTR was found to play no role in the acidification of lysosomes in pancreatic epithelial cells (50). More recently, Deretic and co-workers (51–53) have reported that endosomes and the Golgi hyperacidify in CF due to defective regulation of organellar sodium transport. Direct evidence indicating that chloride is the major counterion in the acidification of endosomes and the Golgi has been obtained using chloride-sensitive fluorophores (17, 18). Evidence from knock-out mice and direct measurements of chloride ion concentration have also indicated a role for the ClC-3 and ClC-5 chloride channels in the acidification of endosomes (54, 55). Synaptic vesicles in ClC-3 knock-out mice also show defective acidification (56). A general role of

ClC proteins in organellar acidification has been challenged, however, as the acidification of lysosomes in neurons is normal in mice with ClC-6 deletion (57) and ClC-7 deletion (58). With regard to the immune system, contradictory evidence for CFTR function in neutrophil phagosomes has been reported (7, 44), and compelling evidence from knock-out mice suggests that ClC-3 activity is necessary for neutrophil function (59). A complete understanding of the molecular determinants of organellar acidification in different tissues, including cells of the immune system, will likely require the combined application of knock-out mice/knockdown technology, highly specific small molecule inhibitors, and selective reporters of ionic content (*i.e.* H^+, Cl^-, K^+, etc., selective probes).

In summary, our findings do not support the contention that phagolysosomal acidification in alveolar macrophages is dependent on CFTR channel activity or that it is impaired in CF. The mechanism of phagosomal acidification proposed by Di *et al.* (7) is also not in accord with our data or precedents in the literature. Because phagolysosomal acidification is central to a proposed mechanism linking defective CFTR chloride channel function with CF lung disease, our results do not support a direct role for CFTR in defective macrophage function in the pathogenesis of CF lung disease. Our findings thus underscore the need for further evaluation of mechanisms such as airway surface liquid dehydration and defective submucosal gland fluid secretion in the pathophysiology of CF.

Acknowledgments—We thank Dr. L. Tradtrantip for isolation of murine alveolar macrophages; Drs. M. A. Matthay, J. W. Lee, and S. Sullivan for providing human alveolar macrophages; and Dr. G. L. Lukacs for helpful discussions.

REFERENCES

1. Ratjen, F., and Doring, G. (2003) *Lancet* **361,** 681–689
2. Rowe, S. M., Miller, S., and Sorscher, E. (2005) *N. Engl. J. Med.* **352,** 1992–2001
3. Verkman, A. S., Song, Y., and Thiagarajah, J. R. (2003) *Am. J. Physiol.* **284,** C2–C15
4. Wine, J. J., and Joo, N. S. (2004) *Proc. Am. Thorac. Soc.* **1,** 47–53
5. Boucher, R. C. (2007) *Trends Mol. Med.* **13,** 231–240
6. Thelin, W. R., and Boucher, R. C. (2007) *Curr. Opin. Pharmacol.* **7,** 290–295
7. Di, A., Brown, M. E., Deriy, L. V., Li, C., Szeto, F. L., Chen, Y., Huang, P., Tong, J., Naren, A. P., Bindokas, V., Palfrey, H. C., and Nelson, D. J. (2006) *Nat. Cell Biol.* **8,** 933–944
8. Delves, P. J., and Roitt, I. M. (2000) *N. Engl. J. Med.* **343,** 37–49
9. Zhang, P., Summer, W. R., Bagby, G. J., and Nelson, S. (2000) *Immunol. Rev.* **173,** 39–51
10. Vieira, O. V., Botelho, R. J., and Grinstein, S. (2002) *Biochem. J.* **366,** 689–704
11. de Jonge, H. R. (2007) *J. Physiol.* (*Lond.*) **580,** 7–8
12. Steinberg, B. E., Touret, N., Vargas-Caballero, M., and Grinstein, S. (2007) *Proc. Natl. Acad. Sci. U. S. A.* **104,** 9523–9528
13. Swanson, J. (2007) *Nat. Cell Biol.* **8,** 908–909
14. Tesciuba, A. G., Subudhi, S., Rother, R. P., Faas, S. J., Frantz, A. M., Elliot, D., Weinstock, J., Matis, L. A., Bluestone, J. A., and Sperling, A. I. (2001) *J. Immunol.* **167,** 1996–2003
15. Lukacs, G. L., Rotstein, O. D., and Grinstein, S. (1990) *J. Biol. Chem.* **265,** 21099–21107
16. Lukacs, G. L., Rotstein, O. D., and Grinstein, S. (1991) *J. Biol. Chem.* **266,** 24540–24548
17. Sonawane, N., Thiagarajah, J. R., and Verkman, A. S. (2002) *J. Biol. Chem.* **277,** 5506–5513
18. Sonawane, N. D., and Verkman, A. S. (2003) *J. Cell Biol.* **160,** 1129–1138
19. Zen, K., Biwersi, J., Periasamy, N., and Verkman, A. S. (1992) *J. Cell Biol.* **119,** 99–110
20. Hackam, D. J., Rotstein, O. D., Zhang, W.-J., Demaurex, N., Woodside, M., Tsai, O., and Grinstein, S. (1997) *J. Biol. Chem.* **272,** 29810–29820
21. Yates, R. M., and Russell, D. G. (2005) *Immunity* **23,** 409–417
22. Ma, T., Thiagarajah, J. R., Yang, H., Sonawane, N. D., Folli, C., Galietta, L. J. V., and Verkman, A. S. (2002) *J. Clin. Investig.* **110,** 1651–1658
23. Gadsby, D. C., Vergani, P., and Csanády, L. (2006) *Nature* **440,** 477–483
24. Guggino, W. B., and Stanton, B. A. (2006) *Nat. Rev. Mol. Cell Biol.* **7,** 426–436
25. Touret, N., Paroutis, P., Terebiznik, M., Harrison, R. E., Trombetta, S., Pypaert, M., Chow, A., Jiang, A., Shaw, J., Yip, C., Moore, H.-P., van der Wel, N., Houben, D., Peters, P. J., de Chastellier, C., Mellman, I., and Grinstein, S. (2005) *Cell* **123,** 157–170
26. Sherry, A. M., Cuppoletti, J., and Malinowska, D. H. (1994) *Am. J. Physiol.* **35,** C870–C875
27. Benharouga, M., Haardt, M., Kartner, N., and Lukacs, G. L. (2001) *J. Cell Biol.* **153,** 957–970
28. Yang, H., Shelat, A. A., Guy, R. K., Gopinath, V. S., Ma, T., Du, K., Lukacs, G. L., Taddei, A., Folli, C., Pedemonte, N., Galietta, L. J. V., and Verkman, A. S. (2003) *J. Biol. Chem.* **278,** 35079–35085
29. Thiagarajah, J. R., Broadbent, T., Hsieh, E., and Verkman, A. S. (2003) *Gastroenterology* **126,** 511–519
30. Biwersi, J., Emans, N., and Verkman, A. S. (1996) *Proc. Natl. Acad. Sci. U. S. A.* **93,** 12484–12489
31. Bradbury, N. A., Jillings, T., Berta, G., Sorscher, E., Bridges, R. J., and Kirk, K. L. (1992) *Science* **256,** 530–532
32. Desjardins, M. (2003) *Nat. Rev. Immunol.* **3,** 280–291
33. Jutras, I., and Desjardins, M. (2005) *Annu. Rev. Cell Dev. Biol.* **21,** 511–527
34. Yates, R. M., Hermetter, A., Taylor, G. A., and Russell, D. G. (2007) *Traffic* **8,** 241–250
35. Nishi, T., and Forgac, M. (2002) *Nat. Rev. Mol. Cell Biol.* **3,** 94–103
36. Desjardins, M., Huber, L. A., Parton, R. G., and Griffiths, G. (1994) *J. Cell Biol.* **124,** 677–688
37. Henry, R. M., Hoppe, A. D., Joshi, N., and Swanson, J. A. (2004) *J. Cell Biol.* **164,** 185–194
38. Kneen, M., Farinas, J., Li, Y., and Verkman, A. S. (1997) *Biophys. J.* **74,** 1591–1599
39. Llopis, J., McCaffery, J. M., Miyawaki, A., Farquhar, M. G., and Tsien, R. Y. (1998) *Proc. Natl. Acad. Sci. U. S. A.* **95,** 6803–6808
40. Lichtman, J. W., and Conchello, J.-A. (2005) *Nat. Methods* **2,** 910–919
41. O'Connor, N., and Silver, R. B. (2007) *Methods Cell Biol.* **81,** 415–433
42. Conchello, J.-A., and Lichtman, J. W. (2005) *Nat. Methods* **2,** 920–931
43. Blocker, A., Severin, F. F., Burkhardt, J. K., Bingham, J. B., Yu, H., Olivo, J.-C., Schroer, T. A., Hyman, A. A., and Griffiths, G. (1997) *J. Cell Biol.* **137,** 113–129
44. Painter, R. G., Valentine, V. G., Lanson, N. A., Leidal, K., Zhang, Q., Lombard, G., Thompson, C., Viswanathan, A., Nauseef, W. M., Wang, G., and Wang, G. (2006) *Biochemistry* **45,** 10260–10269
45. Barsch, J., Kiss, B., Prince, A., Saiman, L., Gruenert, D., and Al-Awqati, Q. (1991) *Nature* **352,** 70–73
46. Biwersi, J., and Verkman, A. S. (1994) *Am. J. Physiol.* **266,** C149–C156
47. Dunn, K. W., Park, J., Semrad, C. E., Gelman, D. L., Shevell, T., and McGraw, T. E. (1994) *J. Biol. Chem.* **269,** 5336–5345
48. Lukacs, G. L., Chang, X.-B., Kartner, N., Rotstein, O. D., Riordan, J. R., and Grinstein, S. (1992) *J. Biol. Chem.* **267,** 14568–14572
49. Seksek, O., Biwersi, J., and Verkman, A. S. (1996) *J. Biol. Chem.* **271,** 15542–15548
50. Van Dyke, R. W., Root, K. V., Schreiber, J. H., and Wilson, J. M. (1992) *Biochem. Biophys. Res. Commun.* **184,** 300–305
51. Poschet, J. F., Skidmore, J., Boucher, J. C., Firoved, A. M., Van Dyke, R. W., and Deretic, V. (2002) *J. Biol. Chem.* **277,** 13959–13965
52. Poschet, J. F., Fazio, J. A., Timmins, G. S., Ornatowski, W., Perkett, E., Delgado, M., and Deretic, V. (2006) *EMBO. Rep.* **7,** 553–559
53. Poschet, J. F., Boucher, J. C., Tatterson, L., Skidmore, J., Van Dyke, R. W., and Deretic, V. (2001) *Proc. Natl. Acad. Sci. U. S. A.* **98,** 13972–13977

54. Hara-Chikuma, M., Wang, Y., Guggino, S. E., Guggino, W. B., and Verkman, A. S. (2005) *Biochem. Biophys. Res. Commun.* **329,** 941–946
55. Hara-Chikuma, M., Yang, B., Sonawane, N., Sasaki, S., Uchida, S., and Verkman, A. S. (2005) *J. Biol. Chem.* **280,** 1241–1247
56. Stobrawa, S. M., Breiderhoff, T., Takamori, S., Engel, D., Schweizer, M., Zdebik, A. A., Bosl, M. R., Ruether, K., Jahn, H., Draguhn, A., Jahn, R., and Jentsch, T. J. (2001) *Neuron* **29,** 185–196
57. Poët, M., Kornak, U., Schweizer, M., Zdebik, A., Scheel, O., Hoelter, S., Wurst, W., Schmitt, A., Fuhrmann, J. C., Planells-Cases, R., Mole, S. E., Hübner, C. A., and Jentsch, T. J. (2006) *Proc. Natl. Acad. Sci. U. S. A.* **103,** 13854–13859
58. Kasper, D., Planells-Cases, R., Fuhrmann, J. C., Scheel, O., Zeitz, O., Ruether, K., Schmitt, A., Poët, M., Steinfeld, R., Schweizer, M., Kornak, U., and Jentsch, T. J. (2005) *EMBO J.* **24,** 1079–1091
59. Moreland, J. G., Davis, A. P., Bailey, G., Nauseef, W. M., and Lamb, F. S. (2006) *J. Biol. Chem.* **281,** 12277–12288